

CONNECTION BETWEEN TRACK GEOMETRY QUALITY AND DYNAMIC VEHICLE RESPONSE AT VARIOUS SPEEDS

CSABA ÁGH*

*Doctoral School of Multidisciplinary Engineering Sciences,
Széchenyi István University, Győr, Hungary*

Received 6 March 2023; accepted 30 May 2023

Abstract. Track geometry measurements are widely used for describing track quality. However, derailments and track deterioration are caused by forces arising in vehicle-track system. This research focuses on two types of vehicle response. Firstly, the influence of the longitudinal level irregularities on the vertical wheel-rail forces was examined. Secondly, the correlation between the lateral axle box acceleration and the cross level irregularities was investigated. Track geometry and vehicle response data were acquired simultaneously by a track recording car, formed from a passenger car, at various speeds up to 130 km/h. Vehicle-track forces were calculated based on accelerometers mounted on the car body, bogies and axle boxes, considering mass and moment of inertia. Non-linear regressions resulted in vertical vehicle-track force estimation functions. It was proven that the use of second spatial derivatives of the longitudinal level gave a better estimation than the use of reference TQIs according to European Standard EN 13848-6. A linear relationship was found between the speed and standard deviation of vertical vehicle-track forces. On straight sections with constant speed, correlation coefficients of around 0.8 were found between second spatial derivatives of cross level and lateral axle box acceleration.

Keywords: axle box acceleration, estimation function, second spatial derivative, track geometry, vehicle response, vehicle-track forces.

* Corresponding author. E-mail: agh.csaba@sze.hu

Csaba ÁGH (ORCID ID 0000-0002-0361-9832)

Copyright © 2023 The Author(s). Published by RTU Press

This is an Open Access article distributed under the terms of the Creative Commons Attribution License (<http://creativecommons.org/licenses/by/4.0/>), which permits unrestricted use, distribution, and reproduction in any medium, provided the original author and source are credited.

Introduction

One of the main tasks of railway maintenance professionals is to prevent derailments. In addition, the track should ensure a defined level of service where important service level indicators are permitted speed and axle load. To maintain the tracks safely and economically, track diagnostics represent a key added value to the infrastructure managers' toolbox. Track geometry measurement data are widely used for describing track quality because of measurability and clarity. However, derailments and further track deterioration are caused by *forces* arising in the vehicle-track system. Forces are triggered, inter alia, by track irregularities. The question could thus be raised whether wheel-rail forces should be measured instead of track geometry. Dynamic wheel-rail forces and accelerations of the vehicle are known hereinafter as a 'vehicle response'. Problem is that there are as many vehicle responses on the same track as there are vehicles. In addition, vehicle response is highly dependent on the speed of the measuring vehicle.

Track geometry data focus on the relative position of rails. The principal parameters of track geometry are longitudinal level, alignment, cross level and gauge (Haigermoser et al., 2015). Other parameters used in track maintenance, such as twist, can be derived from the aforementioned principal parameters.

In the literature, vehicle response is represented by vehicle-track forces or vehicle accelerations. Luber et al. (2010) proposed transfer functions to estimate vehicle-track forces based on the track geometry. Yang et al. (2021) focused on car body accelerations and Dumitriu et al. (2020) focused on bogie vibrations. Costa et al. (2023) investigated the relationships between track quality and safety quantities such as derailment coefficient or wheel unloading. Wang et al. (2023) investigated vertical track irregularities from the perspective of train operation stability on a bridge. According to the categorization of the European standard EN 13848-6 "Characterisation of Track Geometry Quality" (European Committee for Standardization, 2020a), the methods based on vehicle response can rely on theoretical models or direct measurements. It should be noted that in addition to vehicle response, there is also a track response in the vehicle-track system, which was investigated by some researchers (El Moueddeb et al., 2022).

Predicted vehicle response, such as track overloading, is important also from the point of view of track structure design. The dynamic factor is derived by the ratio of the dynamic wheel load to the static wheel load. Van Dyk et al. (2017) and Lee et al. (2020) show more than ten different types of methods for existing dynamic factor calculation such as the

well-known Eisenmann method or the Sadeghi method. There is no consensus among theories even on the influence of speed.

Dedicated track recording cars can have high operation costs and need trained personnel as well as careful planning not to interfere with regular rail traffic. To overcome these obstacles, onboard monitoring of vehicle response via in-service trains was proposed by many papers with a view toward automation (Weston et al., 2015; Hoesl et al., 2022; Vinkó et al., 2023). The ongoing UIC project “Harmotrack” tries to define representative indicators of track quality based on vehicle responses for improved network maintenance and simulation purposes.

The vehicle-track system is extremely complex and has a lot of nonlinear internal contacts. Therefore, vehicle response estimation based on track geometry quality is not straightforward, not even the axle box accelerations. Karis et al. (2020) found that the results show a high correlation coefficient between the vertical axle box acceleration and the second spatial derivative of the longitudinal level when analysing the simulated data, but not for the measured data. The situation of wheel-track forces appears even more challenging because vehicle-track forces compensate the sum of dynamical movements of all components of the vehicle with different acceleration behaviour: wheelsets, bogie frames and car body.

1. Methodology

This paper focuses on the following vehicle responses:

- dynamic part of the vertical wheel-rail force depending on longitudinal level irregularities;
- dynamic part of the lateral axle box acceleration depending on cross level irregularities.

1.1. Investigation of vertical forces acting on the track

The impact of vertical track quality and speed on the vertical vehicle-track forces was investigated. Input data were recorded during test runs made by track recording car “FMK-007” (details about this car can be found in Section 1.3). Used measurement parameters were: longitudinal level (LL), vertical wheel-rail forces at each wheel of the leading wheelset (Q_1, Q_2) and vehicle speed (v).

The results were evaluated over 200 m long sections. The sections were considered without overlap. The values characterising the section were calculated as standard deviation (in case of longitudinal level and vertical vehicle-track forces) or average value (in case of speed).

Although the spatial band-pass filters according to European Standard EN 13848-1 (European Committee for Standardization, 2019) significantly distort the true shape of the isolated defects (Ágh, 2021), in order to compare data of different measuring systems, 'D1' wavelength range of longitudinal level was considered in this paper. Li et al. (2012), Karis et al. (2020) and Ágh (2019) demonstrated the importance of second spatial derivatives by estimating vehicle response. Therefore, vertical track irregularities were considered in two different ways:

- standard deviation of measured D1 longitudinal level: $\sigma(LL)$;
- standard deviation of second spatial derivative of D1 longitudinal level: $\sigma(LL'')$.

It is worth noting that, according to European standard EN 13848-6 (European Committee for Standardization, 2020a), calculating $\sigma(LL)$ is taken as the reference method ($\sigma(LL) = TQI_{ref}$) to describe track geometry quality because of its wide use across European Railway Networks. In contrast, calculating $\sigma(LL'')$ is proposed only by this paper.

The second spatial derivative of the longitudinal level was calculated as follows:

$$LL''(x) = LL(x - \Delta x) - 2 \cdot LL(x) + LL(x + \Delta x), \quad (1)$$

where x is the longitudinal coordinate of the track (railway chainage) and Δx is the differentiation step, which was always 0.75 m. The unit of both LL and LL'' is millimeter. A differentiation step of 0.75 m, proposed by Ágh (2019), was used because this step length resulted in the best correlation with the vehicle response of the FMK-007 measurement car in the investigated speed range. For simplicity, Equation (1) does not take into account the differentiation step.

Standard deviations were calculated for both rails and the average value of the two standard deviations was calculated. The speed of each 200-m-sections was calculated as the average speed of the actual segment.

The vertical dynamical force was considered in two different ways:

- the standard deviation of measured vertical axle load: $\sigma(Q_{ax})$;
- the standard deviation of measured vertical left and right wheel loads: $\sigma(Q_{wh})$.

The expected values of the vertical axle and wheel loads are the static loads mentioned in the Section 1.3. The standard deviation of measured left and right wheel loads were calculated only on straight sections because cant deficiency and cant excess can modify the expected value and standard deviation of both inside and outside rail loads significantly. Therefore, to focus only on the effect of track irregularities, curves and transitions were filtered out. Axle load was calculated as twice the average of the measured left and right wheel loads. Axle load was

considered also on such sections which contained transitions and curves, not only on straight sections because extra wheel load and unload in curves compensated each other. Results are presented in Section 2.1.

1.2. Investigation of lateral axle box acceleration

The impact of the cross level and speed on the lateral axle box acceleration was investigated. Input data were recorded during test runs made by the track recording car “FMK-007”. Used measurement parameters were: cross level (CL), lateral axle box acceleration at the leading wheelset (\ddot{y}_{12}), curvature (G) and vehicle speed (v).

Ágh (2019) demonstrated the importance of the second spatial derivative of cross level by estimating lateral axle box acceleration. Therefore, vehicle response was considered as the second spatial derivative of cross level. The second spatial derivative of the cross level was calculated as follows:

$$CL''(x) = CL(x - \Delta x) - 2 \cdot CL(x) + CL(x + \Delta x), \quad (2)$$

with differentiation step of $\Delta x = 0.75$ m. The used differentiation step of 0.75 m was proposed by Ágh (2019) because this step length resulted in the best correlation with the vehicle response of the FMK-007 measurement car in the investigated speed range. For simplicity, Equation (2) does not take into account the differentiation step.

In order to calculate the correlation with track geometry, the lateral axle box acceleration, which was originally recorded with a sampling

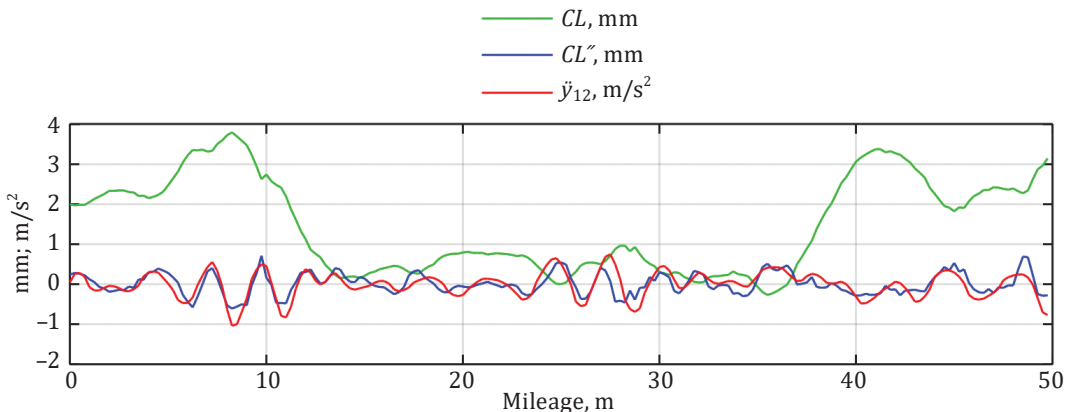


Figure 1. Measured cross level (green), second spatial derivative of cross level (blue) and measured lateral axle box acceleration (red) on straight track at a speed of 127 km/h

rate of 300 Hz, was resampled with a spatial resampling step of 0.25 m. During resampling, a high-precision synchronization was made. Figure 1 shows an example of the original cross level, the second spatial derivative of cross level and the synchronized lateral acceleration.

The correlation of the synchronized results was calculated over 50 m long sections. The 50 m sections were considered with overlap at every sampling step of 0.25 m. The correlation coefficient was calculated between CL'' and \ddot{y}_{12} . The correlation coefficient was investigated in light of the speed and curvature. Results are presented in Section 2.2.

1.3. Measurement setup

Hungarian track recording car “FMK-007” of MÁV Central Rail and Track Inspection Ltd (MÁV KfV Kft.) carried out the test runs. ‘FMK-007’ was converted from a passenger car, which complied with International Coach Regulations (RIC). Its length between buffers is 26.4 m and its total weight is 54 tons (axle loads are around 140 kN); maximum permitted speed of the coach is technically 250 km/h and during regular measurements it is 160 km/h.

FMK-007 is equipped with two separate measuring systems operating in parallel (Ágh, 2018).

On the one hand, it is equipped with a track geometry measuring system in accordance with European standard EN 13848-2 (European Committee for Standardization, 2020b). The data collection units of the track geometry measuring system (Figure 2) consist of six lasers (versine system) and an inertial measurement unit (IMU). According to EN 13848-1 (European Committee for Standardization, 2019), longitudinal level versine values are decoloured (in order to eliminate the influence of transfer function depending on chord lengths) and filtered to the D1 wavelength domain ($3\text{ m} < \lambda \leq 25\text{ m}$).

On the other hand, FMK-007 is also equipped with a vehicle dynamics measurement system based on 24 accelerometer sensors, 20 of which

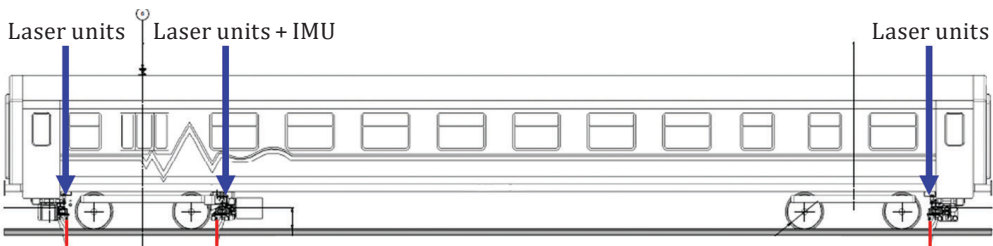


Figure 2. Track geometry measurement system

were used for the calculations presented in this paper. Figure 3 shows the placement of the vertical and lateral sensors on the car body, bogies and axleboxes. Figure 4 shows the method of the attachment of the bogie sensors and axle box sensors.

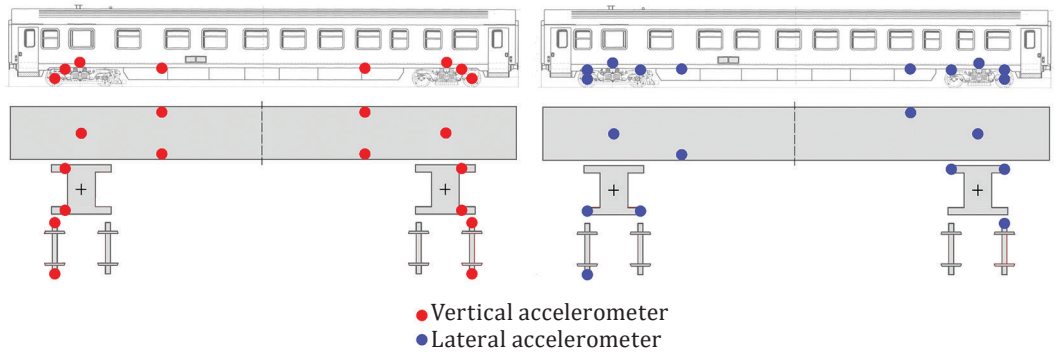


Figure 3. Vertical and lateral accelerometer sensors mounted on FMK-007 measuring car

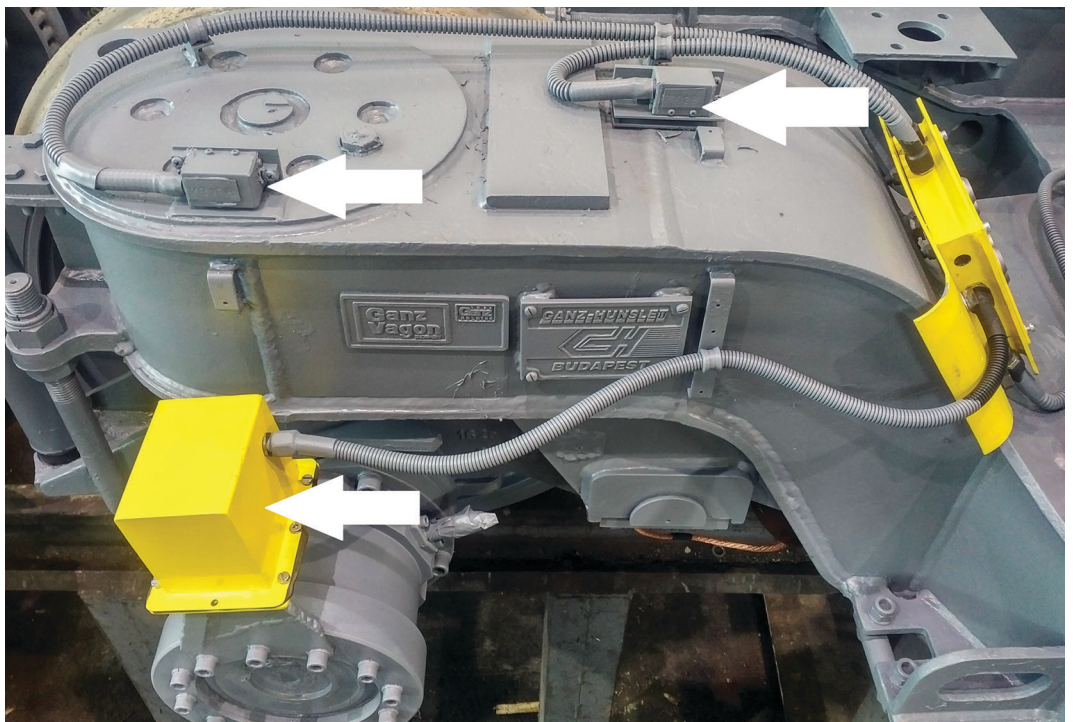


Figure 4. Accelerometer sensor boxes (marked by white arrows) mounted on axlebox and on bogie frame of FMK-007 measuring car

The system was designed according to the “indirect WRIM method”, which was developed by MÁV Research and Development Institute (MÁV FKI), Hungary, in 1998. A detailed description of the method was published by Császár & Pálfi (2013).

Based on Newton’s law, the accelerations of the wheelset can be calculated based on the dynamic wheel-rail contact forces and the axle-box forces. Thus, if both of them are known, the dynamic wheel-rail contact forces can be determined with the help of the inertial and geometrical parameters of the wheelset. In the following formulae and figures of this chapter (Császár & Pálfi, 2013), upper indices ⁺ and ^{*} refer to bogie and car body, respectively (no upper index refers to wheelset). According to Figures 5 and 6, *M* refers to mass, Θ refers to the moment of inertia and *a*, *b*, *r* refer to geometrical distances. Special distances marked with the letter ϑ , for positioning several accelerometer sensors, were calculated with the help of related moment of inertia, according to Császár & Pálfi (2013) and Ágh (2018). The parameters c_s^+ and c_s^* are the vertical distance of the wheelset axle to the gravity centre of the bogie and the car body, respectively. The letters \ddot{y} and \ddot{z} are the measured accelerations and $\ddot{\phi}$ refers to angular acceleration. Vertical wheel-rail forces of leading wheelset $Q_{wh,1}$ and $Q_{wh,2}$, which are shown in Figure 5 as Q_1 and Q_2 , and vertical axle load Q_{ax} are calculated as follows:

$$Q_{wh,1} = \frac{F_{z1} + F_{z2} - M \cdot \ddot{z}}{2} + \left(\frac{F_{z1} - F_{z2}}{2} - \frac{\Theta_x \cdot \ddot{\phi}_x}{2b^+} \right) \cdot \frac{b^+}{b_a} + \frac{r}{2b_a} \cdot \Sigma Y, \quad (3)$$

$$Q_{wh,2} = \frac{F_{z1} + F_{z2} - M \cdot \ddot{z}}{2} - \left(\frac{F_{z1} - F_{z2}}{2} - \frac{\Theta_x \cdot \ddot{\phi}_x}{2b^+} \right) \cdot \frac{b^+}{b_a} - \frac{r}{2b_a} \cdot \Sigma Y, \quad (4)$$

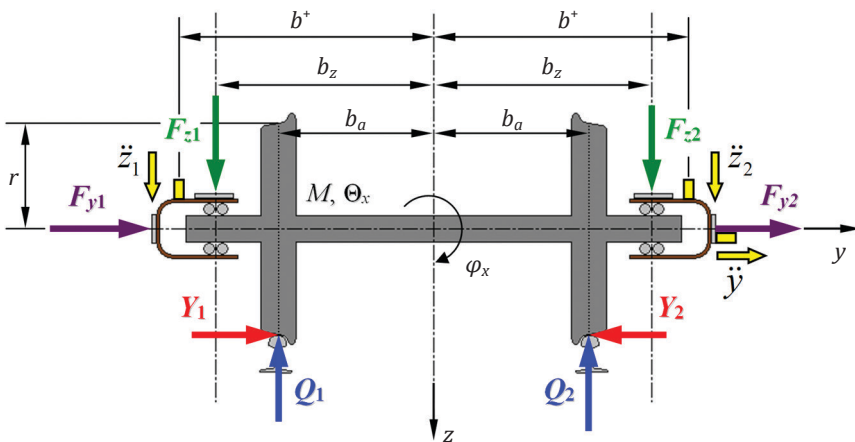


Figure 5. Forces and accelerations acting on the wheelset (Császár & Pálfi, 2013).

$$Q_{ax} = Q_{wh,1} + Q_{wh,2} = F_{z1} + F_{z2} - M \cdot \ddot{z}, \quad (5)$$

where the sum of lateral forces acting on the track is

$$\Sigma Y = Y_1 \pm Y_2 = \Sigma F_{yi} - M \cdot \ddot{y}, \quad (6)$$

and accelerations were calculated from sensor results as follows:

$$\ddot{z} = \frac{\ddot{z}_1 + \ddot{z}_2}{2}, \quad (7)$$

$$\ddot{\phi} = \frac{\ddot{z}_1 - \ddot{z}_2}{2b_z}. \quad (8)$$

In order to determine the forces acting on the wheelset arising from car body and bogie, the following formulae (Császár & Pálfi, 2013) were used, according to Figure 6.

For lateral axle box forces:

$$\Sigma F_y = k_y^* \cdot (-\ddot{y}_0^*) + k_{y1}^+ \cdot (-\ddot{y}_{12}^+) + k_{y2}^+ \cdot (-\ddot{y}_{22}^+), \quad (9)$$

where the geometrical and inertial constants k should be calculated as follows:

$$k_y^* = \frac{M^*}{4}, \quad (10)$$

$$k_{y1}^+ = \frac{M^+}{4} + \frac{\Theta_z^+}{4(a^+)^2}, \quad (11)$$

$$k_{y2}^+ = \frac{M^+}{4} - \frac{\Theta_z^+}{4(a^+)^2}. \quad (12)$$

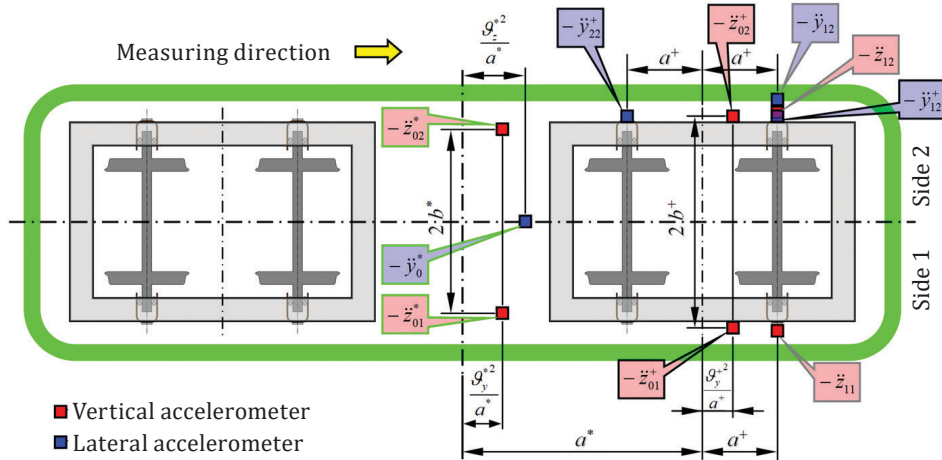


Figure 6. Accelerometers operating parallelly in one measuring direction and the calculation method (Császár & Pálfi, 2013)

Calculation of vertical axle box forces considering inertial forces and moments of bogie and car body:

$$F_{z11} = k_{z1}^* \cdot (-\ddot{z}_{01}^*) + k_{z2}^* \cdot (-\ddot{z}_{02}^*) + k_{z1}^+ \cdot (-\ddot{z}_{01}^+) + k_{z2}^+ \cdot (-\ddot{z}_{02}^+) + k_{zy}^* \cdot F_{y1}^* + k_{zy}^+ \cdot F_{y1}^+, \quad (13)$$

$$F_{z12} = k_{z2}^* \cdot (-\ddot{z}_{01}^*) + k_{z1}^* \cdot (-\ddot{z}_{02}^*) + k_{z2}^+ \cdot (-\ddot{z}_{01}^+) + k_{z1}^+ \cdot (-\ddot{z}_{02}^+) - k_{zy}^* \cdot F_{y1}^* - k_{zy}^+ \cdot F_{y1}^+, \quad (14)$$

where the geometrical and inertial constants k should be calculated as follows:

$$k_{z1}^* = \frac{M^*}{16} + \frac{\Theta_x^*}{16 \cdot b^* \cdot b^+}, \quad (15)$$

$$k_{z2}^* = \frac{M^*}{16} - \frac{\Theta_x^*}{16 \cdot b^* \cdot b^+}, \quad (16)$$

$$k_{z1}^+ = \frac{M^+}{8} + \frac{\Theta_x^+}{8 \cdot b^{+2}}, \quad (17)$$

$$k_{z2}^+ = \frac{M^+}{8} - \frac{\Theta_x^+}{8 \cdot b^{+2}}, \quad (18)$$

$$k_{zy}^* = \frac{c_s^*}{2b^+}, \quad (19)$$

$$k_{zy}^+ = \frac{c_s^+}{2b^+}. \quad (20)$$

The measuring range of axle box accelerometers is 100 g and the measuring range of accelerometers mounted on bogies and car body is 30 g. The sampling rate of all accelerometer sensors is 300 Hz. All accelerometer sensors are uniaxial and made by Brüel & Kjær, connected to MGCplus data acquisition system. Acceleration data were filtered by a 2nd-order low-pass Butterworth filter with a cutoff frequency of 16 Hz. Comparing the aforementioned sampling rate and cutoff frequency with the ones commonly used in vehicle running behavior tests, the following findings can be made based on the European standard EN 14363:2016 "Testing and Simulation for the Acceptance of Running Characteristics of Railway Vehicles" (European Committee for Standardization, 2016). The used sampling rate of 300 Hz is higher than the minimum sampling frequency of 200 Hz proposed by EN 14363. The used cutoff frequency of 16 Hz is similar to the 20 Hz proposed by EN 14363:2016 for vertical wheel forces. Evaluation and further calculations were made via Octave software.

1.4. Test runs

Test runs were carried out on four different railway lines in Hungary. One of the four railway lines is a regional line with fish-plated track

and the other three lines are parts of international corridors with a continuously welded track. All tracks are ballasted and the nominal gauge is overall 1435 mm. The measuring car was hauled by locomotive type “MÁV M61”, maximum running speed was 130 km/h.

During the investigation of the impact of track quality and speed on the vertical *axle* load, 2398 consecutive 200-m-sections were considered, which represented 479.6 km of track. During the investigation of the impact of track quality and speed on the vertical *wheel* load, 1432 sections of 200 m length were considered, which represented 286.4 km of track.

During the investigation of the impact of cross level on lateral axle box acceleration, two international railway lines were selected from the aforementioned railway lines and an 18-km long (test section A) and a 40-km long part (test section B) of them were used for the synchronization. Hence, 72001+159898 overlapping 50-m-sections (with an offset step of 0.25 m) were chosen and synchronized precisely, which represented 58 km of track.

2. Results

2.1. Investigation of vertical forces acting on the track

Based on the test runs made by the aforementioned wagon “FMK-007”, the associated values of vertical track irregularity ($\sigma(LL'')$ or $\sigma(LL)$), speed (v) and vertical vehicle response ($\sigma(Q_{ax})$ or $\sigma(Q_{wh})$) were plotted (marked with red circles on Figures 7 and 8).

Due to the examination of subsets of the results (e.g., Figures 9 and 10), it was found that there was a linear relationship between speed and standard deviation of vertical vehicle-track loads. However, it was found that there was a non-linear relationship between speed and standard deviation of the investigated longitudinal level parameters. Therefore, the following general regression scheme was used:

$$\sigma(Q_j) = \alpha \cdot v \cdot \left[\sigma(LL^{(k)}) \right]^\beta + \varepsilon, \quad (21)$$

where Q_j stands for Q_{wh} or Q_{ax} , $LL^{(k)}$ stands for LL or LL'' , the variables α and β were iterated in order to minimize the residuals ε . For the iteration, mean square error (MSE) of the residuals was minimized and plotted on Figures 7 and 8. Results of the iterations are the following.

The standard deviation of the axle load of FMK-007 wagon over 200 m length sections can be estimated by the formulae:

$$\sigma(Q_{ax}) = 0.029v \cdot [\sigma(LL)]^{2/3} + \varepsilon_1, \quad (22)$$

$$\sigma(Q_{ax}) = 0.058v \cdot [\sigma(LL'')]^{3/4} + \varepsilon_2, \quad (23)$$

where the units of Q , v and LL are kN, km/h and mm, respectively. The static axle load was 140 kN. Surfaces of the aforementioned estimations are shown in Figure 7. The mean square error for the estimations based on Equations (22) and (23) are 0.55 kN^2 and 0.38 kN^2 , respectively. It can be seen that in the case of estimation based on LL'' the points fit better on the surface.

a) based on the standard deviation of longitudinal level

b) based on the second spatial derivative of longitudinal level

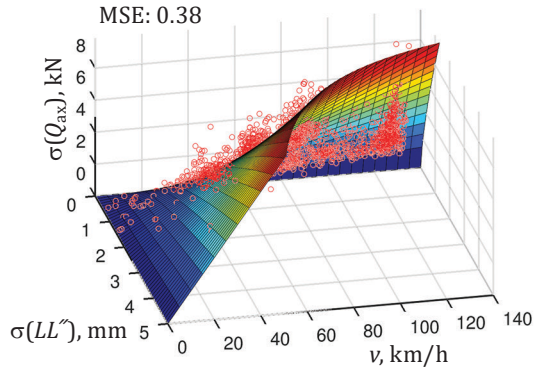
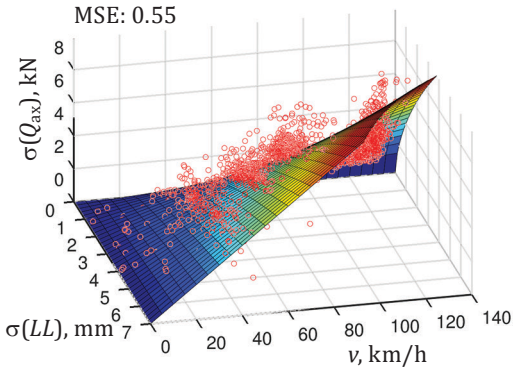


Figure 7. Regression surfaces for estimation of the standard deviation of axle load

a) based on the standard deviation of longitudinal level

b) based on the second spatial derivative of longitudinal level

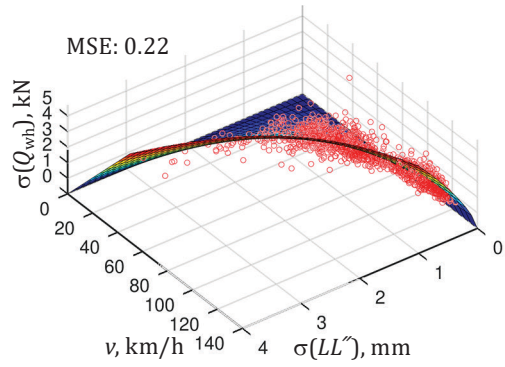
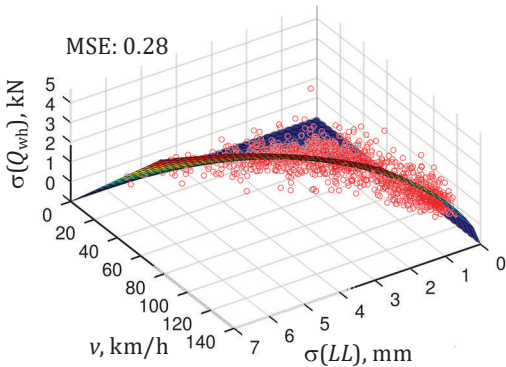


Figure 8. Regression surfaces for estimation of the standard deviation of wheel loads

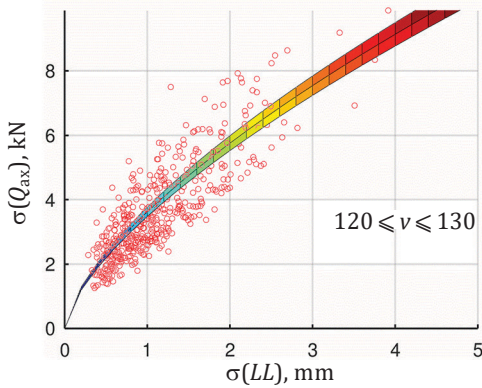
The standard deviation of the wheel load of FMK-007 wagon over 200 m length sections (on straight tracks without curves and transitions) can be estimated by the formulae:

$$\sigma(Q_{wh}) = 0.020v \cdot [\sigma(LL)]^{2/3} + \varepsilon_3, \quad (24)$$

$$\sigma(Q_{wh}) = 0.040v \cdot [\sigma(LL'')]^{3/4} + \varepsilon_4, \quad (25)$$

where the units of Q , v and LL are kN, km/h and mm, respectively. The static wheel load was 70 kN. Surfaces of the aforementioned estimations

a) based on the standard deviation of longitudinal level



b) based on the second spatial derivative of longitudinal level

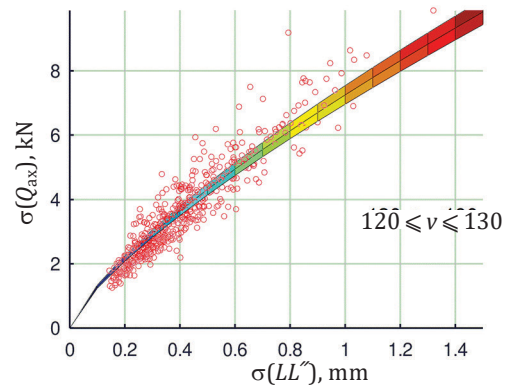
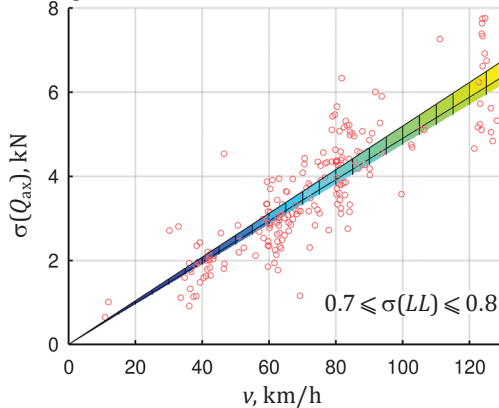


Figure 9. Regression surfaces for estimation of the standard deviation of axle loads in the measurement speed range of 120 km/h to 130 km/h

a) based on the standard deviation of longitudinal level



b) based on the second spatial derivative of longitudinal level

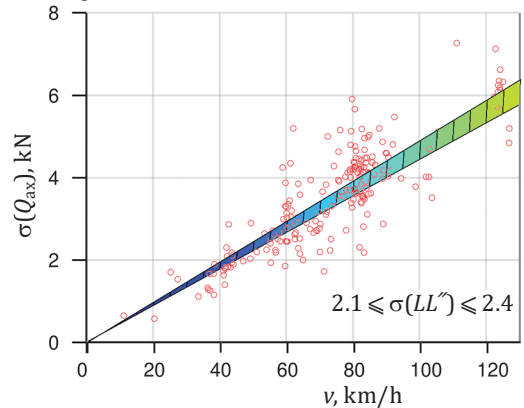


Figure 10. Regression surfaces for estimation of the standard deviation of axle loads in the ranges of LL , mm, and LL'' , mm, written in the figure

are shown in Figure 8. The mean square error for the estimations based on Equations (24) and (25) are 0.28 kN^2 and 0.22 kN^2 , respectively.

Subsets of the dataset and the associated piece of the aforementioned axle load estimation surfaces are shown in the following figures. Figure 9 shows the effect of longitudinal level on the vertical vehicle response over a given speed range (120 km/h to 130 km/h). Figure 10 shows the effect of the speed on the vertical vehicle response over a given track quality range.

Kolmogorov-Smirnov normality tests showed that neither longitudinal level nor wheel load was normally distributed.

2.2. Investigation of lateral axle box acceleration

The correlation coefficient was calculated between the second spatial derivative of the cross level (CL'') and lateral axle box acceleration of the leading wheelset (\ddot{y}_{12}) at each measurement step of the chosen sections of two railway lines. Figures 11 and 12 show the calculated correlation coefficients and the corresponding speed and curvature data. The correlation coefficient was investigated in light of speed and curvature.

The speed of test run A presented in Figure 11 was almost constant. The values of the correlation coefficient were around 0.8. Curves and braking of the train had a significant reducing effect on the correlation coefficient.

The speed of the test run B presented in Figure 12 was variable. The value of the correlation coefficient was over 0.7 in the case of straight track and speeds above 80 km/h. Curves, lower speeds, braking of the train and accelerations had a significant reducing effect on the correlation coefficient.

Conclusions

The research proposed a framework to model relationships between track quality and the standard deviation of dynamic vertical wheel-rail forces. To measure the dynamic wheel-rail forces, an indirect measurement method was proposed, which was based on 20 accelerometer sensors mounted on car body, bogies and wheelsets.

It was found that the standard deviation of vertical vehicle response of the investigated car was determined by the standard deviation of the second order derivative of longitudinal level to a power of 0.75. The standard deviation of vertical vehicle response can also be estimated based on the standard deviation of longitudinal level to a power of 0.66. However, it was proven that the use of second spatial derivatives

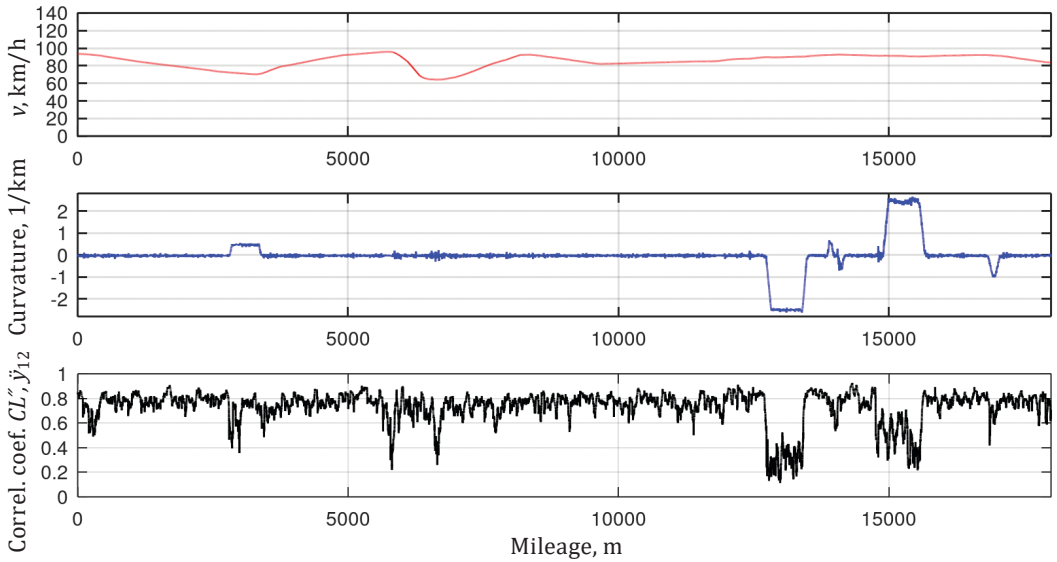


Figure 11. Influence of speed (top) and curvature (middle) on the correlation coefficient (bottom) between the second spatial derivative of the cross level and lateral axle box acceleration along test section A

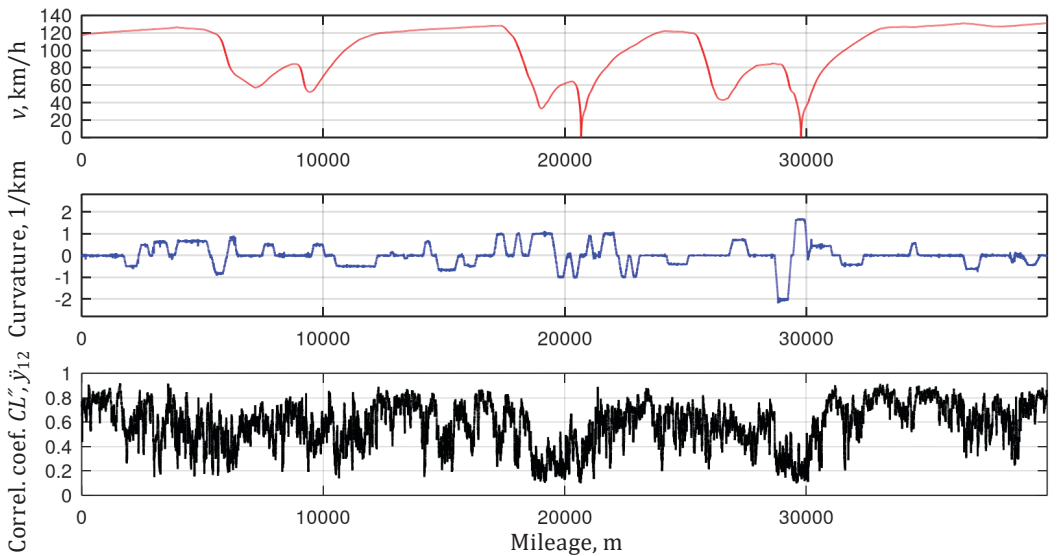


Figure 12. Influence of speed (top) and curvature (middle) on the correlation coefficient (bottom) between the second spatial derivative of cross level and lateral axle box acceleration along test section B

of track geometry data gave a better estimation. It should be mentioned that the estimation method based on the standard deviation of the longitudinal level proposed by this research is important because of the fact that, according to European standard EN 13848-6, the standard deviation of the longitudinal level was taken as the reference method to describe track geometry quality because of its wide use across European Railway Networks. It should be noted that the cutoff frequencies of the used standard filter for longitudinal level (D1) and the used low-pass filter for measured accelerations (16 Hz) can influence the correlation coefficients.

A linear relationship was found between the speed and standard deviation of vertical vehicle-track forces, which depended on the track quality. The examined speed range was limited (up to 130 km/h); therefore, conclusions for higher speeds might not be drawn. However, linearity corresponds to many practical methods for dynamic factor calculation listed by Lee et al. (2020): the method of Eisenmann, Clarke, Sadeghi, Talbot, Indian Railways and South African Railways. In contrast, it should be noted that the German Railways, the method of ORE/Birmann, WMATA method use non-linear speed functions for dynamic factor calculation.

The influence of track quality on axle load deviations and wheel load deviations was similar. However, values of iterated coefficient values α show that the relative deviations from static loads in the case of wheel load deviations are one and a half times higher than in the case of axle load deviations. This fact meets the expectations because wheel load deviations are triggered by both cross level and longitudinal level irregularities. Axle load deviations, which are considered as the averages of wheel load deviations, are not influenced by cross level.

Based on the results, it can be stated that lateral acceleration of passenger cars' axle boxes is significantly influenced by cross level of the track, especially by the second spatial derivative of cross level. On straight sections with constant speed of 80..130 km/h, correlation coefficients of around 0.8 were found between second spatial derivatives of cross level and lateral axle box acceleration. It should be noted that differentiation step (which was 0.75 m in this research) of cross level and cutoff frequency of the used low-pass filter (which was 16 Hz in this research) can have an influence on correlation coefficients at different speeds and different track quality.

As the lateral axle box acceleration contributes to the sum of the lateral wheel-rail forces, it can be stated that cross level deviations jeopardize track quality (and the safety against derailment) also by increasing the lateral force acting upon the rail and wheel, not only by decreasing the vertical force acting upon the rail and wheel.

It should be highlighted that the presented results and formulae refer directly to the car that was tested in this research. However, it can be assumed that the aforementioned results and conclusions can be applied, *mutatis mutandis*, to passenger wagons like the car that was tested in this research. The results can be used in the field of automatized onboard monitoring of vehicle response via in-service trains.

ACKNOWLEDGEMENTS

The author thanks *MÁV Central Rail and Track Inspection Ltd* and *MÁV Zrt.* for enabling the use of the measurement data for research purposes.

DISCLOSURE STATEMENT

No potential conflict of interest was reported.

REFERENCES

- Ágh, C. (2018). A new arrangement of accelerometers on track inspection car FMK-007 for evaluating derailment safety. *Proceedings of 23rd International Seminar "Track Maintenance Machines in Theory and Practice", SETRAS, Žilina, Slovakia*, 7–14.
- Ágh, C. (2019). Comparative analysis of axle box accelerations in correlation with track geometry irregularities. *Acta Technica Jaurinensis*, 12(2), 161–177. <https://doi.org/10.14513/actatechjaur.v12.n2.501>
- Ágh, C. (2021). Measurement distortion analysis of repetitive and isolated track geometry irregularities. *Periodica Polytechnica Civil Engineering*, 65(3), 852–865. <https://doi.org/10.3311/ppci.17638>
- Costa, J. N., Ambrósio, J., Andrade, A. R., & Frey, D. (2023). Safety assessment using computer experiments and surrogate modeling: Railway vehicle safety and track quality indices. *Reliability Engineering & System Safety*, 229, Article 108856. <https://doi.org/10.1016/j.res.2022.108856>
- Császár, L., & Pálfi, C. (2013). Determination of wheel-rail contact forces using different measurement methods. *Proceedings of the 9th International Conference on Railway Bogies and Running Gears*, Budapest, Hungary, 153–166.
- Dumitriu, M., Gheți, M. A., & Cruceanu, I. C. (2020). Experimental analysis of the vertical vibration of the railway bogie during braking. *Procedia Manufacturing*, 46, 49–54. <https://doi.org/10.1016/j.promfg.2020.03.009>

- El Moueddeb, M., Louf, F., Boucard, P. A., Dadié, F., Saussine, G., & Sorrentino, D. (2022). An efficient numerical model to predict the mechanical response of a railway track in the low-frequency range. *Vibration*, 5(2), 326–343. <https://doi.org/10.3390/vibration5020019>
- European Committee for Standardization. (2016). *EN 14363 – Railway applications – Testing and Simulation for the acceptance of running characteristics of railway vehicles – Running Behaviour and stationary tests*. Brussels, Belgium. <https://standards.iteh.ai/catalog/standards/cen/56417fef-6427-4f10-ae76-e01157e2ae93/en-14363-2016>
- European Committee for Standardization. (2019). *EN 13848-1 – Railway applications – Track – Track geometry quality – Part 1: Characterization of track geometry*. Brussels, Belgium. <https://standards.iteh.ai/catalog/standards/cen/19848cc1-08a5-44aa-96aa-18294c6ab12f/en-13848-1-2019>
- European Committee for Standardization. (2020a). *EN 13848-6 – Railway applications – Track – Track geometry quality – Part 6: Characterisation of track geometry quality*. Brussels, Belgium. <https://standards.iteh.ai/catalog/standards/cen/9c85a71e-0f1f-4825-b983-08b9aef34d6e/en-13848-6-2014a1-2020>
- European Committee for Standardization. (2020b). *EN 13848-2 – Railway applications – Track – Track geometry quality – Part 2: Measuring systems – Track recording vehicles*. Brussels, Belgium. <https://standards.iteh.ai/catalog/standards/cen/60b191d2-eb23-4b4e-b5d1-55166df8ed49/en-13848-2-2020>
- Haigermoser, A., Lubner, B., Rauh, J., & Gräfe, G. (2015). Road and track irregularities: measurement, assessment and simulation. *Vehicle System Dynamics*, 53(7), 878–957. <https://doi.org/10.1080/00423114.2015.1037312>
- Hoelzl, C., Dertimanis, V., Landgraf, M., Ancu, L., Zurkirchen, M., & Chatzi, E. (2022). On-board monitoring for smart assessment of railway infrastructure: a systematic review. *The Rise of Smart Cities*, 223–259. <https://doi.org/10.1016/b978-0-12-817784-6.00015-1>
- Karis, T., Berg, M., & Stichel, S. (2020). Analysing the correlation between vehicle responses and track irregularities using dynamic simulations and measurements. *Proceedings of the Institution of Mechanical Engineers, Part F: Journal of Rail and Rapid Transit*, 234(2), 170–182. <https://doi.org/10.1177/0954409719840450>
- Lee, J., Oh, K., Park, Y., & Choi, J. (2020). Study on the applicability of dynamic factor standards by comparison of spring constant based dynamic factor of ballasted and concrete track structures. *Applied Sciences*, 10(23), Article 8361. <https://doi.org/10.3390/app10238361>
- Li, M., Persson, I., Spännar, J., & Berg, M. (2012). On the use of second-order derivatives of track irregularity for assessing vertical track geometry quality. *Vehicle System Dynamics*, 50(sup1), 389–401. <https://doi.org/10.1080/00423114.2012.671947>
- Lubner, B., Haigermoser, A., & Grabner, G. (2010). Track geometry evaluation method based on vehicle response prediction. *Vehicle System Dynamics*, 48(sup1), 157–173. <https://doi.org/10.1080/00423111003692914>

- Van Dyk, B. J., Edwards, J. R., Dersch, M. S., Ruppert Jr, C. J., & Barkan, C. P. (2017). Evaluation of dynamic and impact wheel load factors and their application in design processes. *Proceedings of the Institution of Mechanical Engineers, Part F: Journal of Rail and Rapid Transit*, 231(1), 33–43.
<https://doi.org/10.1177/0954409715619454>
- Vinkó, Á., Simonek, T., Ágh, C., Csikós, A., & Figura, B. (2023). Feasibility of onboard smartphones for railway track geometry estimation: sensing capabilities and characterization. *Periodica Polytechnica Civil Engineering*, 67(1), 200–210. <https://doi.org/10.3311/ppci.20187>
- Wang, M., Yang, C., Ning, B., Li, X., & Wang, P. (2023). Influence mechanism of vertical dynamic track irregularity on train operation stability of long-span suspension bridge. *Proceedings of the Institution of Mechanical Engineers, Part F: Journal of Rail and Rapid Transit*, 237(8), 1037–1049.
<https://doi.org/10.1177/09544097221148794>
- Weston, P., Roberts, C., Yeo, G., & Stewart, E. (2015). Perspectives on railway track geometry condition monitoring from in-service railway vehicles. *Vehicle System Dynamics*, 53(7), 1063–1091.
<https://doi.org/10.1080/00423114.2015.1034730>
- Yang, Y., Liu, G., & Liu, C. (2021). Fine interrelation between track irregularities and vehicle responses: multi-scale time-dependent correlation analysis. *Vehicle System Dynamics*, 59(8), 1171–1189.
<https://doi.org/10.1080/00423114.2020.1741653>